

# Pulse characterization by THG d-scan in absorbing nonlinear media

Mathias Hoffmann,<sup>1,\*</sup> Tamas Nagy<sup>1,2</sup>, Thomas Willemsen,<sup>3</sup> Marco Jupé,<sup>3</sup> Detlev Ristau,<sup>3</sup> and Uwe Morgner<sup>1,3</sup>

<sup>1</sup>*Institute of Quantum Optics, Leibniz Universität Hannover, Welfengarten 1, 30167 Hannover, Germany*

<sup>2</sup>*Laser-Laboratorium Göttingen e.V., Hans-Adolf-Krebs-Weg 1, 37077 Göttingen, Germany*

<sup>3</sup>*Laser Zentrum Hannover e.V., Hollerithallee 8, 30419 Hannover, Germany*

\*[hoffmann@iqo.uni-hannover.de](mailto:hoffmann@iqo.uni-hannover.de)

**Abstract:** We report on few-cycle pulse characterization based on third harmonic generation dispersion scan (THG d-scan) measurements using thin films of different TiO<sub>2</sub>-SiO<sub>2</sub> compositions as nonlinear media. By changing the TiO<sub>2</sub> concentration in the thin film the band gap and therefore the position of the absorption edge were varied. The retrieved pulse durations from different nonlinear media agree within 5%, and the reconstructed pulse shapes prove to be immune against the absorption edges as well. The reason is the robust retrieval algorithm which takes the influence of wavelength dependent nonlinearity into account by a spectral weight function.

©2014 Optical Society of America

OCIS codes: (320.7100) Ultrafast measurements; (320.7110) Ultrafast nonlinear optics.

---

## References and links

1. T. Brabec and F. Krausz, "Intense few-cycle laser fields: Frontiers of nonlinear optics," *Rev. Mod. Phys.* **72**(2), 545–591 (2000).
2. F. Krausz and M. Ivanov, "Attosecond physics," *Rev. Mod. Phys.* **81**(1), 163–234 (2009).
3. C. Iaconis and I. A. Walmsley, "Spectral phase interferometry for direct electric-field reconstruction of ultrashort optical pulses," *Opt. Lett.* **23**(10), 792–794 (1998).
4. D. J. Kane and R. Trebino, "Characterization of arbitrary femtosecond pulses using frequency-resolved optical gating," *IEEE J. Quantum Electron.* **29**(2), 571–579 (1993).
5. V. V. Lozovoy, I. Pastirk, and M. Dantus, "Multiphoton intrapulse interference. IV. Ultrashort laser pulse spectral phase characterization and compensation," *Opt. Lett.* **29**(7), 775–777 (2004).
6. V. V. Lozovoy, B. Xu, Y. Coello, and M. Dantus, "Direct measurement of spectral phase for ultrashort laser pulses," *Opt. Express* **16**(2), 592–597 (2008).
7. B. Hou, J. H. Easter, J. A. Nees, Z. He, A. G. R. Thomas, and K. Krushelnick, "Compressor optimization with compressor-based multiphoton intrapulse interference phase scan (MIIPS)," *Opt. Lett.* **37**(8), 1385–1387 (2012).
8. M. Miranda, T. Fordell, C. Arnold, A. L'Huillier, and H. Crespo, "Simultaneous compression and characterization of ultrashort laser pulses using chirped mirrors and glass wedges," *Opt. Express* **20**(1), 688–697 (2012).
9. M. Miranda, C. L. Arnold, T. Fordell, F. Silva, B. Alonso, R. Weigand, A. L'Huillier, and H. Crespo, "Characterization of broadband few-cycle laser pulses with the d-scan technique," *Opt. Express* **20**(17), 18732–18743 (2012).
10. B. Alonso, M. Miranda, Í. J. Sola, and H. Crespo, "Spatiotemporal characterization of few-cycle laser pulses," *Opt. Express* **20**(16), 17880–17893 (2012).
11. A. Harth, M. Schultze, T. Lang, T. Binhammer, S. Rausch, and U. Morgner, "Two-color pumped OPCPA system emitting spectra spanning 1.5 octaves from VIS to NIR," *Opt. Express* **20**(3), 3076–3081 (2012).
12. T. Y. F. Tsang, "Optical third-harmonic generation at interfaces," *Phys. Rev. A* **52**(5), 4116–4125 (1995).
13. T. Tsang, M. A. Krumbügel, K. W. Delong, D. N. Fittinghoff, and R. Trebino, "Frequency-resolved optical-gating measurements of ultrashort pulses using surface third-harmonic generation," *Opt. Lett.* **21**(17), 1381–1383 (1996).
14. S. K. Das, C. Schwanke, A. Pfuch, W. Seeber, M. Bock, G. Steinmeyer, T. Elsaesser, and R. Grunwald, "Highly efficient THG in TiO<sub>2</sub> nanolayers for third-order pulse characterization," *Opt. Express* **19**(18), 16985–16995 (2011).
15. F. Silva, M. Miranda, S. Teichmann, M. Baudish, M. Massicotte, F. Koppens, J. Biegert, and H. Crespo, "Near to mid-IR ultra-broadband third harmonic generation in multilayer graphene: few-cycle pulse measurement using THG dispersion-scan," in *CLEO Europe* (2013), CWH1.5.

16. R. R. Nair, P. Blake, A. N. Grigorenko, K. S. Novoselov, T. J. Booth, T. Stauber, N. M. R. Peres, and A. K. Geim, "Fine structure constant defines visual transparency of graphene," *Science* **320**(5881), 1308 (2008).
  17. M. Lappschies, B. Görtz, and D. Ristau, "Application of optical broadband monitoring to quasi-rugate filters by ion-beam sputtering," *Appl. Opt.* **45**(7), 1502–1506 (2006).
  18. W. H. Press, S. A. Teukolsky, W. T. Vetterling, and B. P. Flannery, *Numerical Recipes: The Art of Scientific Computing*, 3rd ed. (Cambridge University, 2007), Chap. 10.5.
  19. O. Stenzel, *The Physics of Thin Film Optical Spectra – An Introduction* (Springer, 2005), Chap. 12.4.2.
  20. C. Dölle, C. Reinhardt, P. Simon, and B. Wellegehausen, "Generation of 100  $\mu$ J pulses at 82.8 nm by frequency tripling of sub-picosecond KrF laser radiation," *Appl. Phys. B* **75**(6-7), 629–634 (2002).
- 

## 1. Introduction

Few-cycle laser pulses find numerous applications in contemporary ultrafast science [1,2]. For the generation and optimization of such pulses the complete characterization of the electric field (amplitude and phase) is essential. For this task various measuring techniques are used, e.g. SPIDER [3], FROG [4] or MIIPS [5–7]. Most of them require rather complex setups, involving interferometers or pulse shapers.

Recently, Miranda *et al.* [8] introduced a novel pulse measurement method: the dispersion scan or d-scan. Here, material dispersion is added gradually to the initially negatively chirped pulse in a way that the pulse is scanned from negative to positive dispersion. In each state nonlinear signals are generated and their spectra are recorded. Although this technique has some limitations [9], it is capable to determine the optimal pulse shape for a given laser/compressor arrangement, which is the most relevant measure for ultrafast light sources. Great advantage of the d-scan technique is its experimental simplicity: in combination with a spectrometer setup only a nonlinear medium, chirped mirrors and glass wedges are needed. The latter two are standard components of any few-cycle ultrafast laser systems.

In [8–10] d-scan measurements of near-IR pulses were presented using second harmonic generation in BBO crystals. However, second-order nonlinearities are not well suited for the characterization of pulses with octave spanning or even broader spectra (e.g [11].) since it is hard to distinguish between the overlapping parts of the fundamental and the generated nonlinear signals. In these cases higher-order nonlinearities can help; employing third harmonic generation (THG) allows the characterization of pulses with spectra spanning up to 1.5 octaves [12–14]. The first demonstration of a d-scan measurement based on higher-order nonlinearity has been reported recently [15], where THG in graphene films was used. Generally, THG suffers from low efficiencies which can be partially compensated by using materials with large nonlinearities (e.g. graphene). Another substantial issue of THG is that the generated short-wavelength radiation can be close to the UV resonances of the nonlinear medium resulting in non-uniform nonlinearity and dispersion. Even graphene which is known to have uniform absorption in broad spectral range becomes increasingly absorbing below 400 nm [16].

The aim of this work is to find out whether near-resonant THG processes can be used in d-scan measurements to reliably retrieve pulse shapes of few-cycle laser pulses. Therefore we performed a set of THG d-scan measurements of pulses from a Ti:sapphire oscillator using ternary Ti/SiO<sub>2</sub> compound layers as nonlinear media where the band gap has been systematically varied by changing the composition. In this way the position of the UV absorption edge and therefore the extent of the overlap between the absorption band and the TH spectrum of the pulses could be changed. We found out that d-scan measurements with significantly different overlaps between the TH spectrum and the absorption band of the nonlinear material delivered consistent results for the retrieved pulse shape. Furthermore, the bigger the overlap was, the higher the THG signal became considerably improving the signal to noise ratio of the measurement.

## 2. Experimental

The schematic of the setup is depicted in Fig. 1: The sub-6 fs pulses of the laser oscillator (VENTEON, Ti:Sa, 80 MHz) are negatively chirped by two double chirped mirrors so that extra material (two fused silica wedges with apex angles of  $2^\circ$ ) is needed to compress the pulses at the sample plane. The beam was focused into the layer on the exit surface of the samples by a reflective objective ( $f = 13$  mm). Co-propagating fundamental and harmonic radiation is separated behind a prism sequence. In performing a d-scan the amount of fused silica in the beam path is changed by small steps ( $70 \mu\text{m}$ ) and the harmonic spectra for each step are recorded by a highly sensitive UV spectrometer (Andor SR-303i-A equipped with a Newton EMCCD (DU970-UV) camera).

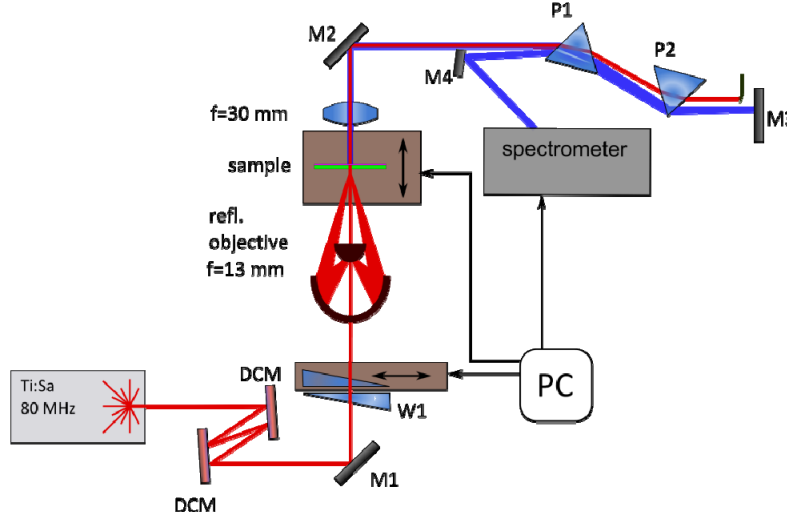


Fig. 1. Experimental setup for THG d-scan. P1, P2: prisms, W1: wedges, DCM: double chirped mirrors, M1-4: mirrors, PC: computer.

The thin films, manufactured on 1 mm thick suprasil substrates by an ion beam sputtering technique specially optimized for ternary material mixtures [17], consist of different compositions of Ti/SiO<sub>2</sub> (with band gaps between 3.26 and 4 eV) and have different optical thicknesses ( $\lambda/16 - 3\lambda @ 780$  nm). Beside these composite films a set of dc-magnetron-sputtered TiO<sub>2</sub> layers and a ZnS (band gap 3.54 eV) layer were also examined. The last one was manufactured by in-house pulsed laser deposition with a q-switched laser source (FWHM 12 ns, 6 W, 1064 nm, 40 kHz, focused onto bulk ZnS target under 40 degree angle to the surface, distance between target and substrate: 40 mm).

In the course of the retrieval process the d-scan trace is simulated ( $S_{\text{sim}}(\omega, z)$ ) by calculating the third harmonic signal of an assumed input pulse constructed from the input spectrum together with a phase curve. The latter is composed of the assumed phase of the input pulse together with the one accumulated in the fused silica wedges of thickness  $z$ . The phase curve is determined by its second derivative [9] at an adaptive number of up to 100 supporting points on the frequency axis. The Nelder-Mead optimization algorithm (see e.g [18].) minimizes the difference between the recorded ( $S_{\text{meas}}(\omega, z)$ ) and simulated d-scans

$$d = \sum_{i,j} \left( S_{\text{meas}}(\omega_i, z_j) - \mu_i(\omega_i) S_{\text{sim}}(\omega_i, z_j) \right)^2 \quad (1)$$

by varying the spectral phase assumption together with a spectral weight function  $\mu(\omega)$  (Eq. (7) in [8]) taking the wavelength dependence of signal generation and detection

efficiency into account [8]. In a usual case the algorithm takes typically 45 minutes for the phase retrieval on a standard PC.

Following [8] the spectral weight function  $\mu(\omega)$  can be separated into two parts: one describes the properties of the setup and the other one is given by the nonlinear coefficient of the medium under test.

$$\mu(\omega) = \mu_{\text{setup}}(\omega) \mu_{\text{NL}}(\omega) \quad (2)$$

With

$$\mu_{\text{setup}}(\omega) = R_{\text{mir}}(\omega) T_{\text{optics}}(\omega) D_{\text{spec}}(\omega) \quad (3)$$

$\mu_{\text{setup}}$  includes the spectral influence of all components after signal generation (reflectivity of mirrors -  $R_{\text{mir}}(\omega)$ , transmission of prisms and lenses -  $T_{\text{optics}}(\omega)$  and diffraction efficiency of the grating and sensitivity of the CCD -  $D_{\text{spec}}(\omega)$ ) while  $\mu_{\text{NL}}$  contains the frequency dependent third-order susceptibility  $\chi^{(3)}(\omega)$  and other effects influencing the signal generation e.g. phase matching and re-absorption in the layer. Due to the use of amorphous materials the third-order susceptibility  $\chi^{(3)}(\omega)$  gets independent of direction and can be approximated as a scalar.

### 3. Results and discussions

In Figs. 2 and 3 measured and reconstructed d-scan traces together with the reconstructed temporal and spectral shapes are depicted for a pure  $\text{TiO}_2$  layer and the ZnS layer, respectively. In both cases the agreement between measured and reconstructed traces is excellent. It is worth noting that in spite of great differences between the appearances of the d-scan traces of the  $\text{TiO}_2$  and ZnS layers, the reconstruction algorithm delivers very similar pulse shapes, and the pulse durations (FWHM) of 5.6 fs and 5.8 fs agree also well.

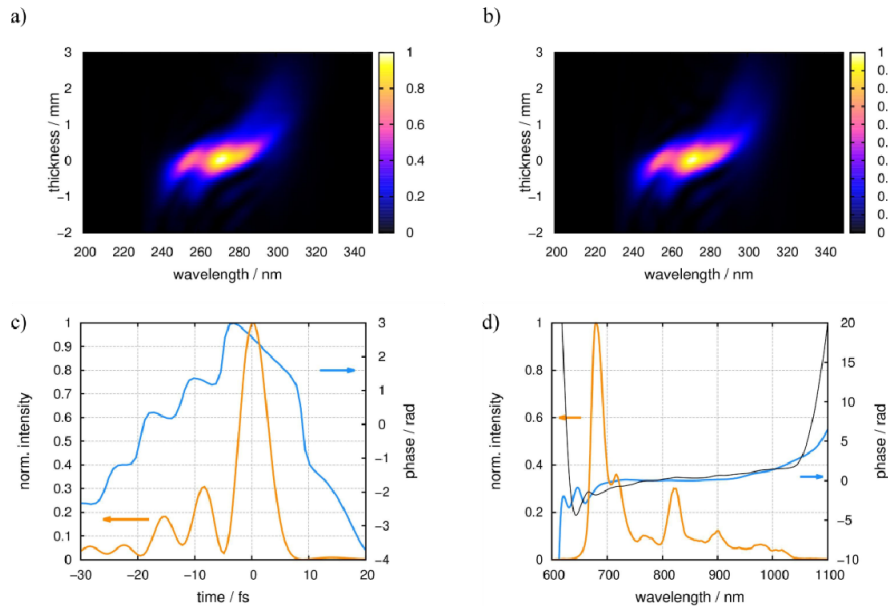


Fig. 2. THG-d-scan measurement using a 21 nm thick  $\text{TiO}_2$  layer: the measured and retrieved traces are shown in (a) and (b), respectively. (c) displays the retrieved pulse shape while (d) depicts the measured spectrum together with the retrieved spectral phase from d-scan (blue) and from SPIDER measurement (black curve).

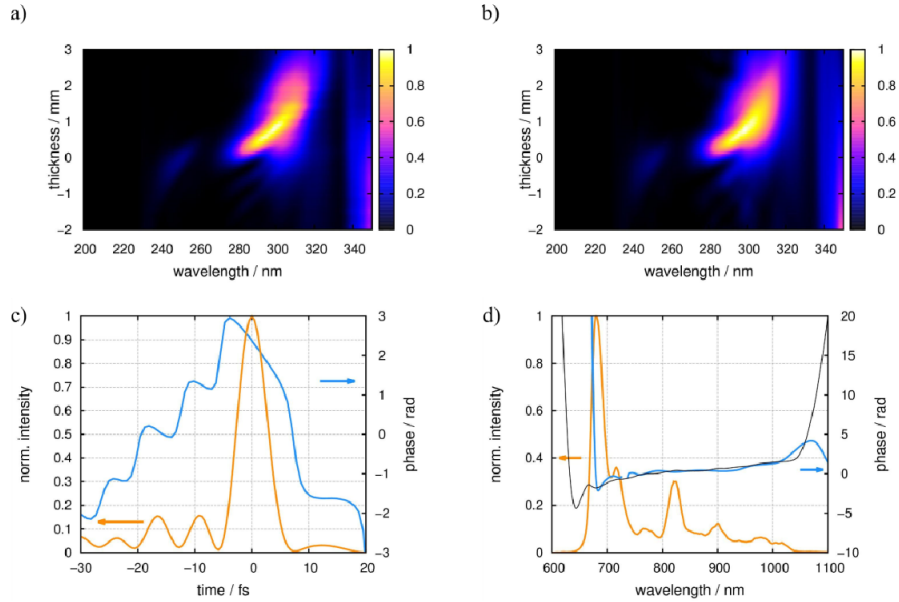


Fig. 3. THG-d-scan measurement using a 300 nm thick ZnS layer.

The reconstructed pulse shapes and pulse durations for all different 28 samples employed for THG are depicted in Figs. 4(a) and 4(b), respectively. For comparison, an independent SPIDER measurement (VENTEON | PULSE: FOUR SPIDER) of the fundamental pulse was taken resulting in an FWHM pulse duration of 5.3 fs. The mean value of the pulse durations of the d-scans is 5.6 fs with a standard deviation of 0.05 fs, which deviates from the SPIDER measurement within 6%. Considering the calibration precision of the SPIDER technique and the error budget of the d-scan (wedge angle, dispersion data, spectrometer calibration) this agreement is remarkably good.

The band gaps for the ion-beam and dc-magnetron sputtered layers are determined with the Tauc method [19]. Energies of 3.2 and 4.0 eV correspond to wavelengths of 387 and 310 nm, respectively. The third harmonic signal is located around 310 nm where the layers are absorbing. As Fig. 4(b) clearly shows the pulse durations are surprisingly independent of the band gap and the sample thickness. In Fig. 5 wavelength dependent absorption measurements for a variety of layers are shown together with a typical third harmonic spectrum.

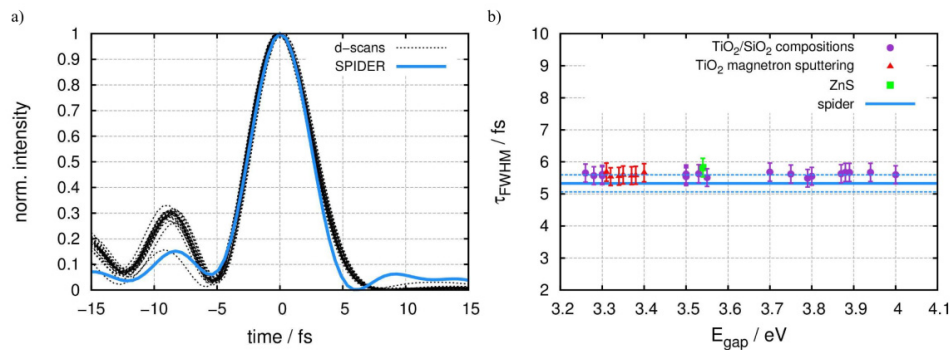


Fig. 4. (a): Reconstructed pulse envelopes of all 28 layers. The thinner dashed black lines represent the d-scan measurements; the thick blue line shows the SPIDER measurement. (b): Pulse durations in function of the band gap with errors of 5%. The line represents the pulse duration of the SPIDER measurement.

Regarding the overlap between the absorption band and the third harmonic spectrum a layer of 21 nm pure  $\text{TiO}_2$  absorbs already 50% at the harmonic wavelengths. As a consequence, the origin of the observed radiation must be very close to the layer surface with perfect phase matching for broadband frequency conversion.

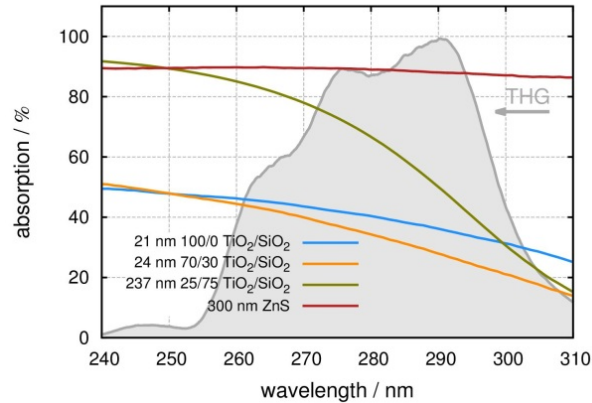


Fig. 5. Absorption of layers of different thicknesses and compositions: 21 nm  $\text{TiO}_2$  (blue), 24 nm  $\text{Ti}_{70}\text{Si}_{30}\text{O}_2$  (orange), 237 nm  $\text{Ti}_{25}\text{Si}_{75}\text{O}_2$  (olive) and 300 nm ZnS (red). A typical THG spectrum is depicted in grey.

In Fig. 6 the maxima of the spectral power densities of TH signals achieved by the samples are displayed in function of the band gap. It is obvious from the graph that the TH signal increases with the overlap between the TH spectrum and the absorption band. This is advantageous by optimizing the signal to noise ratio and therefore the quality of the d-scan measurement. In the particular case of our laser pulse the highest signal was achieved by a pure  $\text{TiO}_2$  layer.

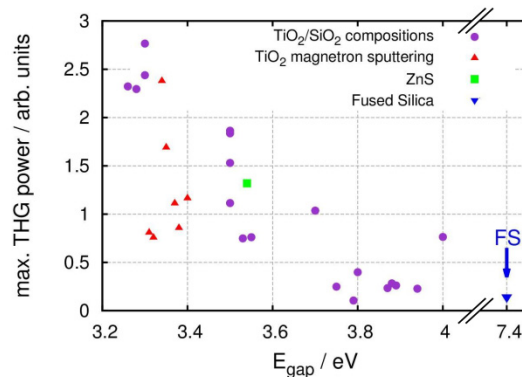


Fig. 6. Peak of the THG signal in function of the band gap.

The retrieval algorithm is capable of extracting the pulses accurately from the different samples by mapping the spectral dependent nonlinearity into the weight function  $\mu(\omega)$  (see Eq. (2)). Since the absorption edge of fused silica is far above the third harmonic spectrum (7.4 eV, 168 nm), it is reasonable to assume that the nonlinearity function is constant over the spectral range considered here. By normalizing the weight functions of the samples by those of fused silica (shown in Fig. 7) the influences of the setup ( $R_{\text{mir}}(\omega)$   $T_{\text{optics}}(\omega)$   $D_{\text{spec}}(\omega)$ ) are factored out, and the resulting function reveals the wavelength dependent nonlinear coefficient (and absorption and phase matching if relevant).

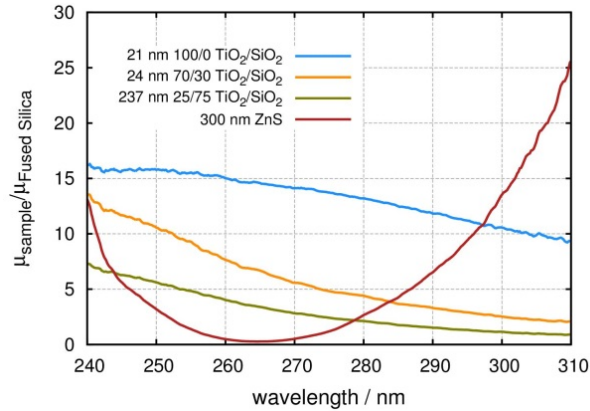


Fig. 7. Normalized spectral weight functions  $\mu_{\text{sample}}(\omega)/\mu_{\text{Fused Silica}}(\omega)$  for 21 nm  $\text{TiO}_2$  (blue), 24 nm  $\text{Ti}_{70}\text{Si}_{30}\text{O}_2$  (orange), 237 nm  $\text{Ti}_{25}\text{Si}_{75}\text{O}_2$  (olive) and 300 nm ZnS (red) layers.

Thanks to the high nonlinearity  $\text{TiO}_2$  and also ZnS can produce considerably higher third harmonic signal than fused silica, although their absorption is significantly higher. In case of ternary mixed  $\text{Ti}_{1-x}\text{Si}_x\text{O}_2$  layers the weight functions increase with decreasing wavelength although the absorption also increases. Obviously, the gain in the THG efficiency due to the resonant nonlinearity overcompensates the absorption losses in the dielectric material in a similar way as it was e.g. observed in resonant THG in gases [20].

#### 4. Conclusion

In this work we present THG-d-scan measurements of sub-6 fs pulses by using  $\text{Ti}_x\text{Si}_{1-x}\text{O}_2$  thin films with band gaps varying between 3.26 and 4 eV. In fact, the generated third harmonic spectra are partially overlapping with the absorption bands of the various nonlinear materials to different extent. Although the recorded d-scan traces show significant differences between different nonlinear materials, the retrieved pulse shapes are very consistent and pulse durations agree within 5% error for all materials independent of the band gap. Reason for this is the robustness of the data retrieval algorithm. It not only minimizes the difference between measured and retrieved d-scan by varying the spectral phase of the input pulse, it also takes the influence of the wavelength dependent nonlinearity with a spectral weight function into account. The harmonic signal is strongly enhanced by the absorbing layer; it is generated at the surface giving rise to perfect phase matching for ultra-broadband spectra, opening up the prospect of proper pulse characterization even for single cycle pulses.

#### Acknowledgments

This work was funded by Bundesministerium für Bildung und Forschung (BMBF, project: PEARLS (13N10155)) and Deutsche Forschungsgemeinschaft within the project “Measuring lifetime and magnitude of the optical Kerr-effect in tailored bandgap materials” (Mo850/16-1). We acknowledge support by Deutsche Forschungsgemeinschaft and Open Access Publishing Fund of Leibniz Universität Hannover.